Geophys. J. Int. (1991) **107**, 171–184

Ordovician magnetostratigraphy: Llanvirn–Caradoc limestones of the Baltic platform

Trond Helge Torsvik* and Allan Trench*
Department of Earth Sciences, University of Oxford, Oxford OX1 3PR, *UK*

Accepted 1991 June 5. Received 1991 June 5; in original form 1991 January 31

SUMMARY

Palaeomagnetic sampling has been performed covering 43 stratigraphic levels within the Baltoscandian Ordovician carbonates. After removing a ubiquitous Permo-Carboniferous (287 ± 14 Ma) remagnetization between 200° and 500 °C, a Llanvirn–Caradoc reversal stratigraphy is delineated by components with maximum unblocking temperatures up to 550°–580 °C. Three reversed (SE, down) and three normal (NW, up) antipodal polarity intervals have been recognized. A primary/early diagenetic remanence age is therefore inferred for the stratigraphically linked polarity chrons. Primary magnetizations are resident in detrital/biogenic or early diagenetically formed single- and pseudo-single domain magnetite phases and subordinate early diagenetic pigmentary haematite.

The recognition of a primary remanence within these well-dated Ordovician carbonates has the following important tectonic and magnetostratigraphic consequences.

(1) Accurate time-calibration of the Baltic APW path implies that rapid counter-clockwise rotation took place in late Tremadoc and Llandeilo times. The Arenig–Llanvirn epochs are characterized by a 'still stand'. Baltica occupied intermediate to high Southerly latitudes during the early Ordovician (Tremadoc–Llanvirn). Systematic northward drift is recognized in post-Llanvirn times.

(2) A time-calibrated Ordovician reversal stratigraphy is proposed. Presently available data suggest the geomagnetic field was predominantly reversely polarized during Tremadoc and Arenig times. Two normal polarity zones of short duration are identified within mid-Llanvirn and mid-Llandeilo strata. Discontinuities within the succession may mask other short-period events. Late Llandeilo to mid-Caradoc times were then characterized by a normal polarity field.

Key words: Baltica, Ordovician magnetostratigraphy, palaeomagnetism, palaeotectonics.

INTRODUCTION

Attempts to delineate the Lower Palaeozoic movement history of Baltica have been hampered by a sparsity of palaeomagnetic data and the tendency for existing data to be dominated by younger overprint magnetizations (Torsvik *et al.* 1990a). Recently, although new data bearing on this problem have become available, the location of these studies within areas of structural complexity has meant that some tectonic uncertainties remain within the derived apparent polar wander path (Torsvik *et al.* 1990b).

* Now both at: Geological Survey of Norway, PB 3006 Lade, N-7002 Trondheim, Norway.

Likewise the definition of a time-calibrated reversal stratigraphy for the Ordovician period has proven difficult. In this respect, many Ordovician data are drawn from either intrusive rocks (e.g. Watts & Briden 1984; Torsvik *et al.* 1990b) or from volcanics of relatively narrow age range (e.g. McCabe & Channell 1990; Trench *et al.* 1991).

In this account, we present a detailed magnetostratigraphic section embracing mid-Llanvirn to mid-Caradoc limestones from Vestergotland, southern Sweden (Fig. 1a—area code 6). Palaeomagnetic results from Swedish Ordovician limestones were first published by Claesson (1978). Although only reverse polarity data with SE declinations (*c.* 132°) and steeply dipping positive inclinations (*c.* 70°) were initially reported, occasional

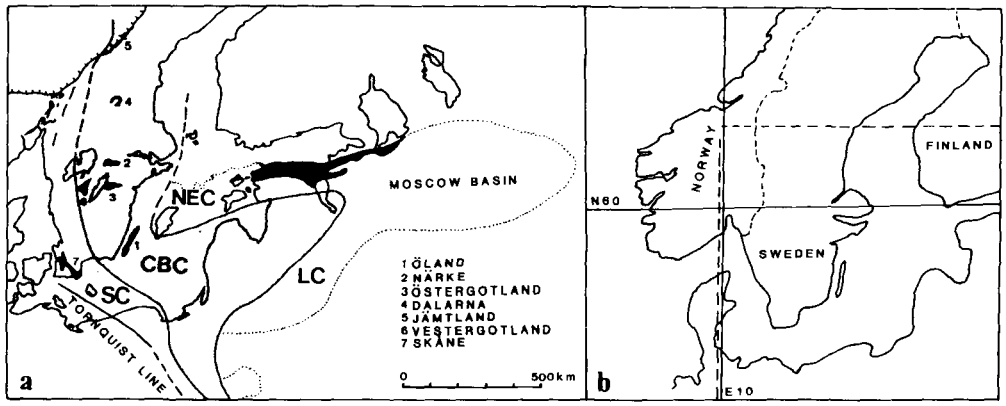

Figure 1. (a) Distribution of Ordovician outcrops in southern Sweden (dark filled areas—numbered 1 to 7; this study concerns area 6, Vestergotland), and Ordovician confacies boundaries. SC = Scanian Confacies Belt; CBC = Central Baltoscandian Confacies Belt; NEC = North Estonian Confacies Belt; LC = Lithuanian Confacies Belt (after Jaanusson 1982a). (b) Southern Scandinavia; the left area of (a) is indicated by stippled lines.

normal polarity directions were present in the original data set of Claesson (1977) (*cf.* Torsvik & Trench 1991). The stratigraphic distribution of these polarity changes therefore warranted further investigation.

GEOLOGICAL BACKGROUND AND SAMPLING DETAILS

Based on faunal and lithological constraints, the Ordovician of Baltoscandia is divided into a number of *confacies* belts (Jaanusson 1976, Fig. 1a). These belts strike approximately N–S in southern Sweden with an easterly tongue toward the Moscow Basin. Facies boundaries, however, changed somewhat with time and transitional zones of varying width frequently developed across adjacent belts (Palma 1967; Jaanusson 1976).

As the combined thickness of Upper Cambrian to Upper Ordovician strata seldom exceeds 150 m, an extremely slow average sedimentation rate (1–3 m Myr^{-1}) is indicated. However, disconformities of considerable magnitude occur

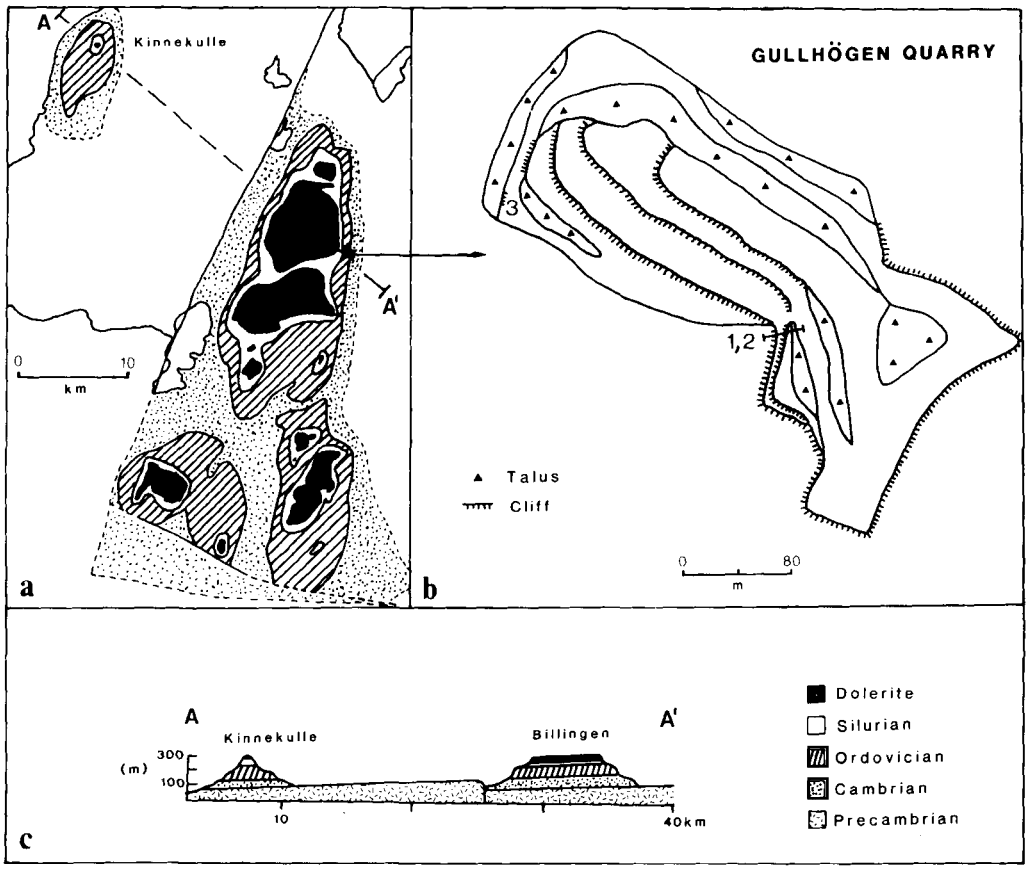

Figure 2. (a) Geological sketch map of the Billingen–Kinnekulle area, Vestergotland [*cf.* legend in (c)—simplified from Jaanusson (1982b)]. (b) Sketch-map of the Gullhögen quarry (after Holmer 1989). Sampling sections 1–3 are indicated. (c) Geological cross-section through profile A–A′ in (a) (simplified from Thorslund 1962).

within the section (e.g. Lindström 1971; Holmer 1983) implying sedimentation to have been somewhat episodic. Whether these periods of non-deposition formed either as submarine hard-grounds or indicate periodic emergence remains contentious (*cf.* Lindström 1971; Jaanusson 1982a; Holmer 1983).

The present study focuses on the Billingen–Falbygden area within the Central Baltoscandian confacies belt (Figs 1 and 2). In this area of Vestergotland, sandstones and shales dominate the Lower and Middle–Upper Cambrian facies, carbonates comprise the Ordovician sequence, and graptolitic shales are prevalent in the Silurian (Jaanusson 1982b). The Cambro-Silurian sequence is flatlying (Fig. 2c) and is capped by a Permo-Carboniferous dolerite sill (287 ± 14 Ma—Mulder 1971). Dolerite sills have served as a protective erosional cover for the Cambro-Silurian sequence and now form prominent topographic features in Vestergotland.

On eastern Billingen, the Gullhögen Quarry at Skøvde (Fig. 2a and b) exposes a continuous section of Upper Cambrian to Upper Ordovician beds of approximately 70 m (Thorslund & Jaanusson 1960; Jaanusson 1964; Jaanusson 1982b; Holmer 1989). In the present study, we describe a stratigraphic survey embracing mid-Llanvirn to mid-Caradoc beds (see stratigraphic subdivisions of the section in Fig. 3). Sampling was concentrated over this time interval as Arenig and Llanvirn limestones have been studied in some considerable detail (Claesson 1977, 1978; Torsvik & Trench 1991; Perroud, Robardet & Bruton 1991).

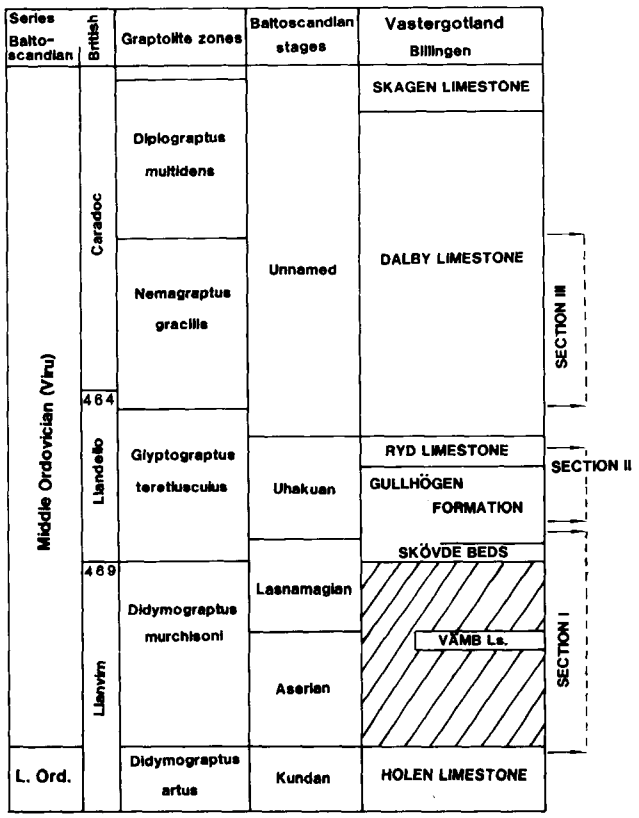

Figure 3. Stratigraphic section for the Vestergotland area (simplified from Holmer 1989). Sampling sections I–III are indicated. Time-scale after Harland *et al.* (1989).

We describe palaeomagnetic data from three sections, delineated in the field by marker horizons within the local stratigraphy (sections I–III in Figs 2b and 3). Unfortunately, due to the inaccessibility of particular quarry faces and to the fissile nature of several shaly facies, some gaps are inevitable. 43 stratigraphic levels were examined (2 to 4 drill-cores from each stratigraphic level) resulting in a total of 145 drill-cores (19 × 19 mm) covering 27 m vertical thickness. Detailed accounts of the geology of Gullhögen Quarry are given by Jaanusson (1982b) and Holmer (1989). Although the precise section locations are likely to be destroyed by quarrying activity, the lithostratigraphy is sufficiently distinctive to allow the appropriate levels to be relocated in future.

Section I (sampling levels 1–14)

Section I (Figs 3 and 4) comprises the upper part of the Holen Limestone (mid-Llanvirn), the Vamb Limestone (mid–upper Llanvirn), the Skövde beds (Lower Llandeilo), and the lower part of the Gullhögen Formation (Lower Llandeilo).

The Holen limestone (levels 1 and 2) comprises well-bedded red and subordinate grey limestones which form part of a widespread litho- and biofacies, referred to as the Orthoceratic limestone. The limestones consist of carbonate mudstones mixed with strata rich in skeletal sands (Kundan Balstoscandian stage—Fig. 3). No major sedimentary breaks have been reported. Sample level 1 was positioned 35 cm below the contact with the Vamb limestone (Fig. 4).

The Vamb limestone (level 3) is approximately 12 cm thick, and is bounded by upper and lower discontinuity surfaces inferred to represent considerable time-gaps (Holmer 1989). Bioturbation at the lower discontinuity surface is extremely rare (Holmer 1983), but 10–20 mm thick bleached zones are occasionally seen below the discontinuity surface. The Vamb limestone contains distinctive red iron-rich ooids and laminated stromatolite structures (Aserian Baltoscandian stage—Fig. 3).

The Skövde beds (level 4) are formed from variegated red and grey limestone of approximately 15 cm thickness. The beds are again bounded by discontinuity surfaces. The Skövde beds form the basal section of the Gullhögen formation (Jaanusson 1982b; Holmer 1989).

The Gullhögen formation (levels 5–14 in section I) reaches *c.* 12.3 m in thickness (including the Skövde beds) consisting of dark calcareous mudstone to fine nodular limestone. Reddish horizons close to the lower boundary of the formation contain ooids (Holmer 1989).

Section II (sampling levels 15–28)

Section II traverses the mid-upper Gullhögen formation (levels 15–22) including a phosphatized discontinuity surface at *c.* 7.5 m. The section continues into the grey-coloured Ryd limestone (levels 23–28), comprising approximately 9 m of thick bedded carbonate mudstones with some minor nodular intercalations. The lower boundary is clearly defined lithologically, whereas the upper is drawn on faunal evidence (Jaanusson 1964; Holmer 1989).

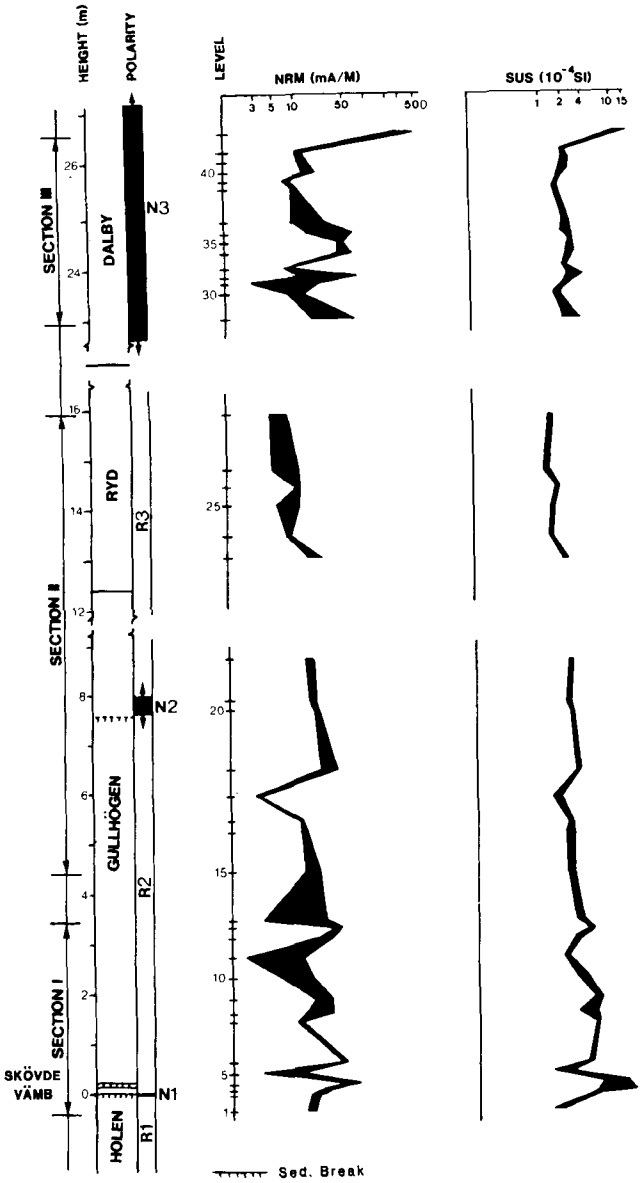

Figure 4. Sampling sections (I–III) and levels (1 to 43), height given in metres, NRM intensities (logarithmic scale), bulk susceptibilities (logarithmic scale) and magnetic polarity zones (N1–N3 and R1–R3).

Section III (sampling levels 29–43)

Section III covers the Dalby Limestone (Upper Llandeilo–mid Caradoc) which has been divided into two members (Holmer 1989). The lower member, (6.3 m, levels 29–43), consists of thickly bedded, grey carbonate mudstones becoming calcarenitic in the upper part. The upper member, (5.5 m), comprises interbedded nodular calcarenites and calcareous mudstones. Only Lower–mid Caradoc limestones of the lower member were sampled.

PALAEOMAGNETIC AND ROCK MAGNETIC EXPERIMENTS

Natural remanent magnetizations (NRM's) were measured on a two-axis Squid magnetometer. Stability of NRM was tested by means of stepwise-thermal and to a lesser extent alternating-field (AF) demagnetization. Characteristic remanence components were calculated interactively using least-square algorithms. Magnetic susceptibilities were measured on a Minisep bulk susceptibility head. Acquisition of isothermal remanent magnetization (IRM), thermal demagnetization of composite IRM, and thermomagnetic analyses were also undertaken.

NRM directions

NRM directions from section I are dominated by SSW and shallow dipping remanences (Fig. 5), but with a distinct girdle distribution toward SE and steeply downward dipping directions, i.e. the characteristic high-blocking direction reported in earlier studies of the Ordovician of Sweden (Claesson 1978; Torsvik & Trench 1991; Perroud *et al.* 1991). In section II, SSW shallow directed components predominate, and finally NRM direction of section III are entirely SSW with shallow negative inclinations, i.e. typical Permo-Carboniferous field directions (Mulder 1971; Torsvik & Trench 1991). NRM directions thus reflect the increased influence of Permo-Carboniferous thermal overprinting upsection in the Ordovician sequence approaching the dolerite sill (Fig. 2a and c).

NRM demagnetization experiments

Demagnetization spectra are thermally distributed up to 550°–580 °C. The NRM is composite, and the majority of samples display three remanence components of contrasting thermal unblocking spectra. First, a poorly resolved

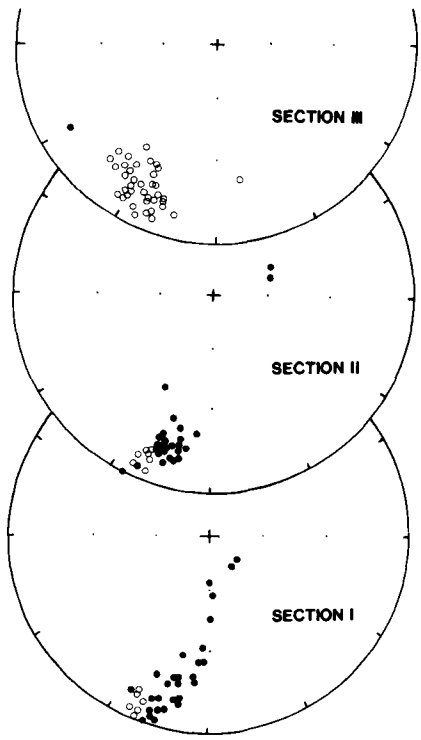

Figure 5. Distribution of NRM directions from sections I–III. Open (closed) symbols in equal-angle stereo-plots denote negative (positive) inclinations.

low-temperature (LB) component is removed up to 150°–200 °C. This component is positively inclined in most samples but is considered too poorly defined for directional analysis. Secondly, a shallow intermediate-temperature (IB) component due SSW is delineated. IB typically unblocks over a temperature range of 200°–500 °C. Finally, a high-temperature (HB) component is identified above 450°–500 °C.

In section I, HB components are of reverse polarity with SE declinations and steep downward dipping inclinations (Fig. 6a). Occasionally, IB components can prove difficult to isolate, and in some instances appear to be composite indicating some overlap of thermal stability between components. In other cases however, the IB component is more easily delineated (Fig. 6b, see also Fig. 8a and b).

AF demagnetization proved inadequate in defining the multicomponent nature of the NRM when samples from the same stratigraphic level are compared using AF and thermal methods (Fig. 7a and b). Although thermal demagnetization indicates the presence of three components (LB, IB, HB) with somewhat overlapping stability spectra in this example (Fig. 7a), AF demagnetization reveals no indication of component HB (Fig. 7b). This behaviour indicates complete overlap of coercivity spectra and AF treatment was therefore discontinued. Coercivity spectra display a correlation with sample colour upon AF demagnetization. Low-coercivity phases are more prominent in grey limestones than variegated red/grey and red limestones respectively (Fig. 7c).

The HB component is more easily defined than the IB components in section I although samples do exhibit considerable viscosity above 520°–530 °C. In most cases however, demagnetization trajectories are linearly decaying toward the origin of the vector diagram below the

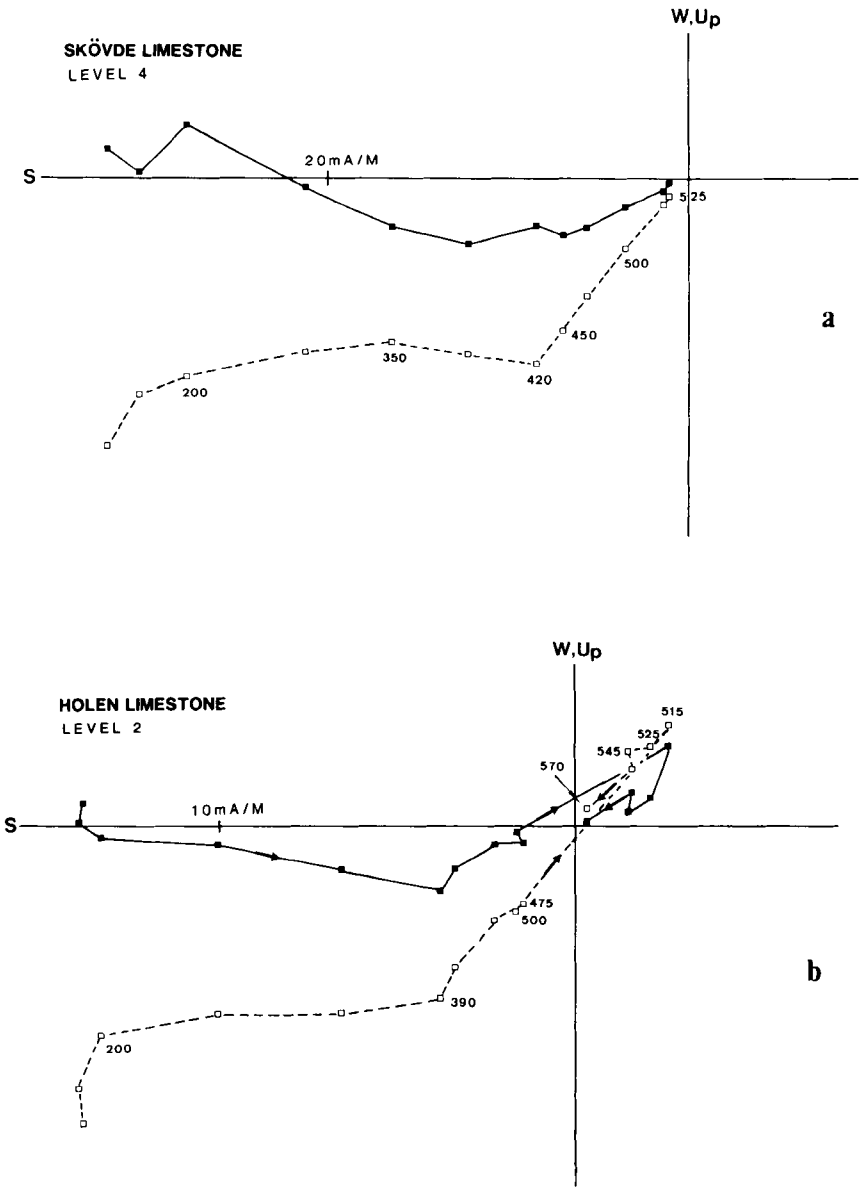

Figure 6. Example of thermal demagnetization of samples from (a) the Skövde and (b) the Holen limestone. In orthogonal vector projections, open (closed) symbols represent points in the vertical (horizontal) plane.

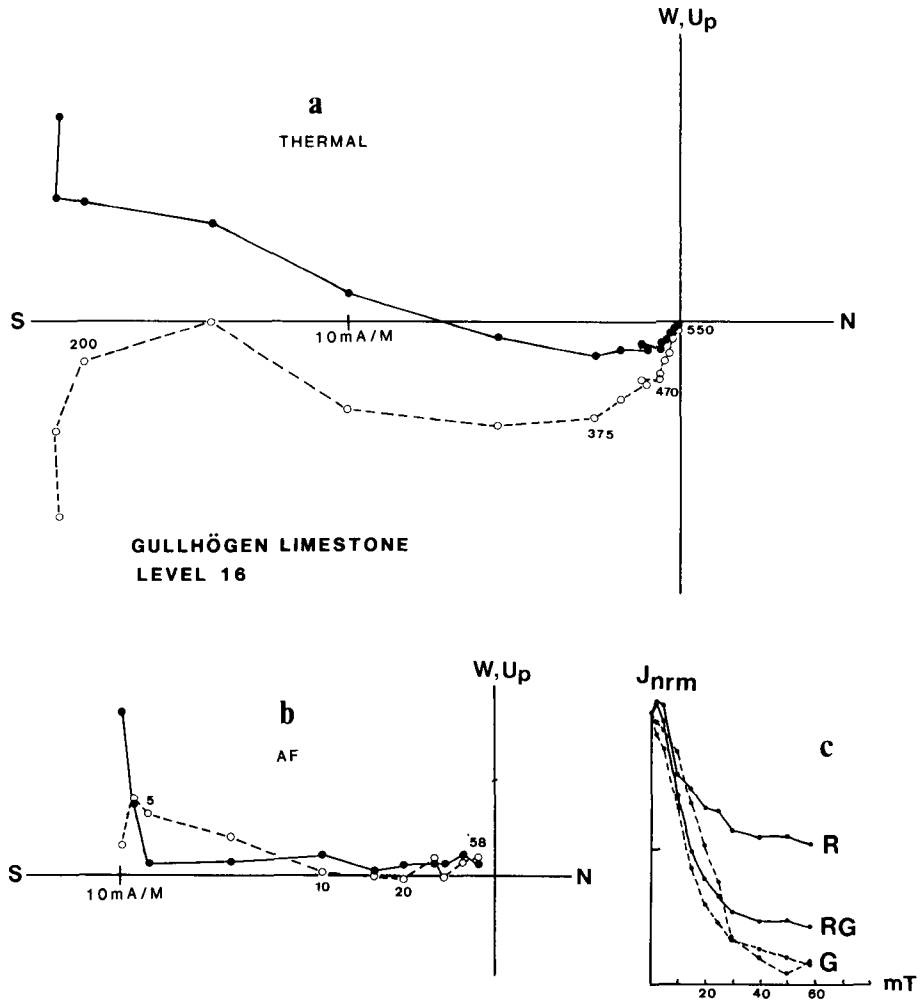

Figure 7. Examples of thermal (a) and AF (b) demagnetization of samples from the Gullhögen limestone. (c) Characteristic AF NRM decay curves (normalized) for red (R), variegated red and grey (RG) and grey (G) limestone.

temperatures at which viscous erratic behaviour commenced (Figs 6a and 7a). Conversely, samples from the Holen limestone indicate that the reverse HB component does not decay to the origin. This suggests the presence of an underlying component which was adequately defined in only one sample (level 2, Fig. 6b). In this case, the IB component is removed between 200° and 390 °C, the reverse HB component between 390° and 515 °C, and finally an antipodal normal polarity HB direction is unblocked between 525° and 570 °C. Both HB components identified in this dark grey limestone appear to reside in magnetite as indicated by the maximum unblocking temperatures and magnetomineralogical experiments (see later). Apart from the top of the Holen limestone, the HB components of section I are exclusively of reverse polarity (zones R1 and R2 in Fig. 4).

Section II, commencing in the Gullhögen Formation, is also of reverse polarity (zone R2), but in reddish mid-Llandeilo limestones normal polarity HB components are present (Fig. 8a). Note that the IB components comprise a larger proportion of the NRM and are much better defined as one progresses up-section (compare Figs 6 and 7 with Fig. 8). Unfortunately, the precise stratigraphic thickness of the normal polarity zone (zone N2) observed in the Gullhögen formation is not determinable since sampling immediately below and above levels 20 and 21 proved difficult (Fig. 4), and a prominent sedimentary break intervenes below stratigraphic level 20. HB components from the top Gullhögen formation and the Ryd limestone (section II) are again of reverse polarity (zone R3).

The Dalby Limestone (section III) is of normal polarity (Fig. 4) although HB components are slightly offset from the origin in the mid–upper part of the formation (Fig. 8b). The identification of any remaining component proved impossible due to viscous behaviour above 545°–550 °C however.

The upper part of section III (levels 42–43) was entirely dominated by the IB component. Complete magnetic overprinting was also occasionally observed within some lower beds, indicating both lithological and distance control on the degree of overprinting by the dolerite sill. Maximum unblocking temperatures of the IB component increase statistically upsection (Fig. 9) demonstrating the increased thermal effects of the overlying sill. Overlapping blocking temperature spectra between components IB and HB (e.g. Figs 6a and 7a) may have mimicked apparent single component behaviour in some samples. This effect can be

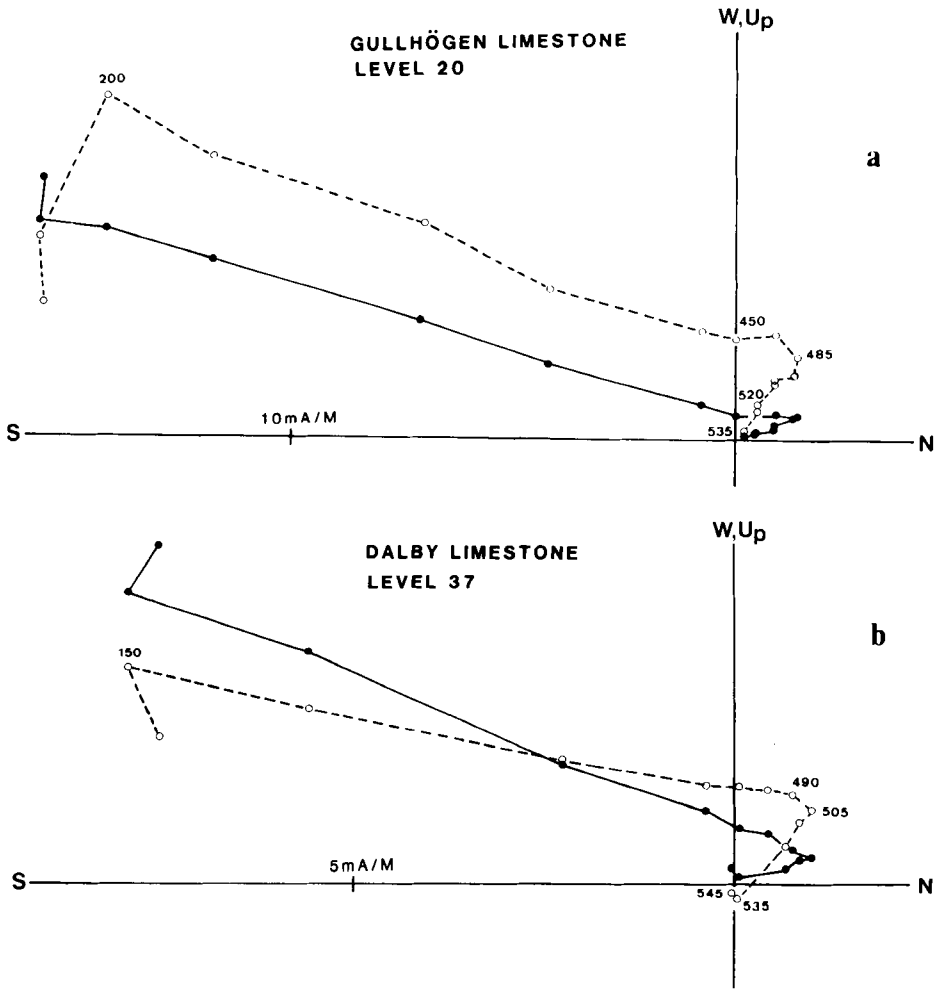

Figure 8. Examples of thermal demagnetization of the Gullhögen (a) and the Dalby limestone (b).

recognized as the direction of the IB components is not identical in sections I–III (Fig. 9). In section III, the inclinations are mostly negative and smear toward the normal polarity HB components seen in this section. Conversely, in sections I and II, we note the increased influence of positively inclined inclinations, now smearing toward the reverse HB directions.

The IB components obtained from the Ordovician limestones yield an overall mean of Dec. = 198 and Inc. = −10, corresponding to a pole position at N35, E171. Despite the problems outlined above, this mean pole compares well with a Permo-Carboniferous (287 ± 14 Ma) palaeomagnetic pole obtained from the overlying Vestergotland dolerite sills (N31 and E174—Mulder 1971).

NRM intensity and bulk susceptibility

NRM intensity and bulk-susceptibility determinations are typically of the order of 5–20 mA m^{-1} and 20–30 (10^{-5} SI units) respectively (Fig. 4). Within sections I and II, the variation in bulk-magnetic properties closely relates to the colouring of the rocks. Grey samples (<5 mA m^{-1}) generally have lower NRM intensities than red/grey samples (*c.* 10–15 mA m^{-1}), which in turn are weaker than red samples (*c.* 20–25 mA m^{-1}). Likewise, grey samples are characterized by lower bulk-susceptibilities. This suggests that total 'iron' (magnetite) content is also lower in grey beds.

In the grey Dalby limestone of section III, variations in NRM intensity are dominated by the effect of the variable Permo-Carboniferous remagnetization. Notably, beds having the highest NRM intensities (up to 500 mA m^{-1}) are completely characterized by the secondary IB components (e.g. levels 34–35 and 43). Bulk-susceptibilities show less variation, suggesting only minor mineralogical changes during overprinting. Note, however, the peak in both NRM intensity and bulk susceptibility at e.g. level 43. This may relate to secondary production of magnetite during heating.

IRM analysis

The presence of both high- and low-coercivity magnetic phases is evident from both AF demagnetization and IRM curves (Figs 7c and 10). In both datatypes, the magnetic properties display a strong correlation with lithological colour.

In this respect, red samples of the Holen and Gullhögen limestones are dominated by high-field phases whereas interbedded grey limestones display a higher proportion of low-field phases. Variegated red and grey limestones

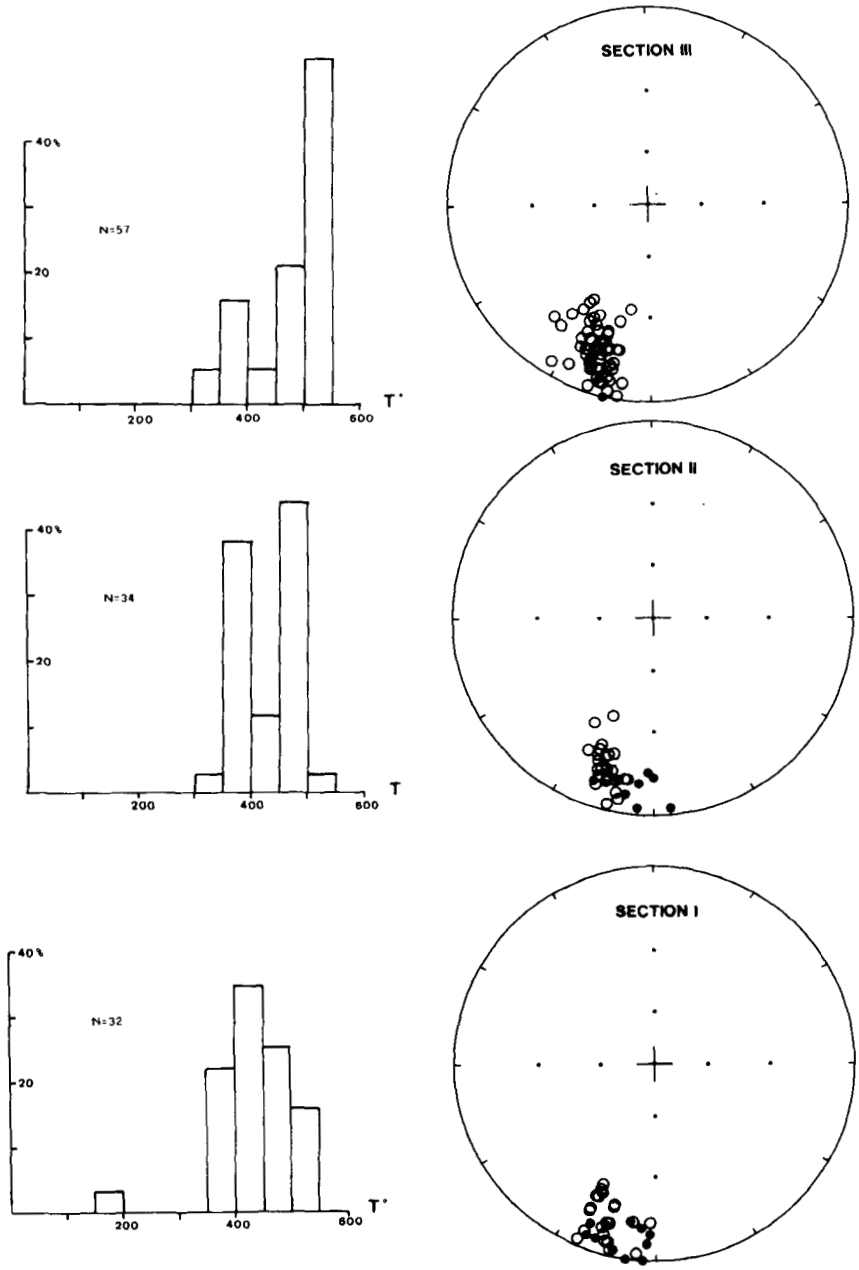

Figure 9. Distribution of IB components from sections I–III (stereo-plots). Histograms show maximum unblocking temperatures for the IB components [percentage frequency along vertical axis—number (*N*) of IB components is indicated for each sections].

accordingly show an intermediate behaviour (Fig. 10a and b). Variegated red/grey and red limestones did not achieve saturation in fields of 0.8 T and *minimum* remanence coercive forces (Hcr) are always in excess of 50 mT.

In the predominantly grey-coloured Ryd limestone, low-field phases dominate but a subordinate high-field contribution is evident (Fig. 11a). Conversely, the grey Dalby Limestone appears entirely governed by low-field phases, indicating a change in magnetic characteristics close to the formation boundary (Fig. 11b). In the Dalby limestone most samples achieved saturation in fields of *c.* 0.3 T and Hcr average to 42 mT. These values suggest the presence of a single- or pseudo-single-domain magnetite fraction.

Composite IRM analysis

Representative samples of varying colour from each formation were chosen for composite IRM analysis. In 10 selected samples, a field of 0.8 T was induced in the *X* axis (horizontal plane) followed by 0.2 T in the *Y* axis (vertical plane). The samples were then stepwise thermally demagnetized. The thermal decay curves of the induced IRM are distributed (Fig. 12d) with approximately *1 per cent* of the initial intensity remaining at 550 °C.

Grey limestone samples from the Dalby formation (section III) show little influence of high-coercivity phases (Fig. 11b). Accordingly, IRM samples show only the low-field induced component (Fig. 12a—example Ag) which

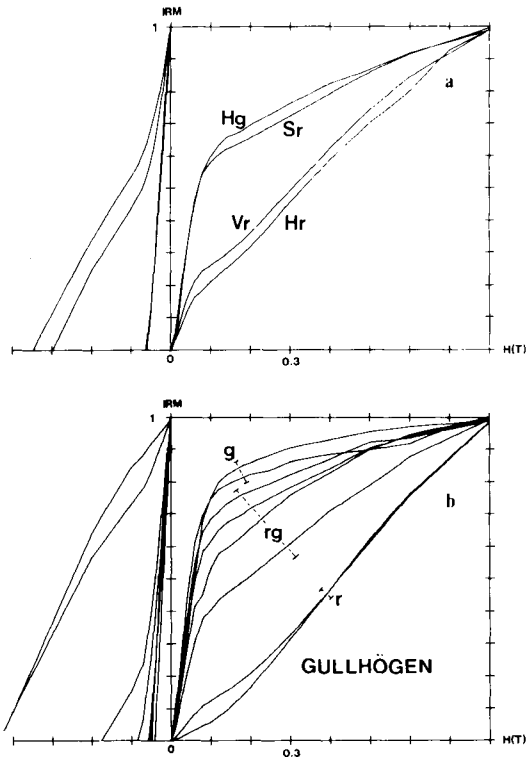

Figure 10. (a) Normalized IRM acquistion curves for the Holen, Skövde and Vamb limestone. Hg = Holen-grey limestone; Sr = Skövde-red limestone; Vr = Vamb-red limestone; Hr = Holen-red limestone. (b) Normalized IRM curves for the Gullhögen limestone. g = grey limestone, rg = variegated red and grey, r = red limestone. H(t) = magnetizing field in Tesla; horizontal axis unit = 0.1 T.

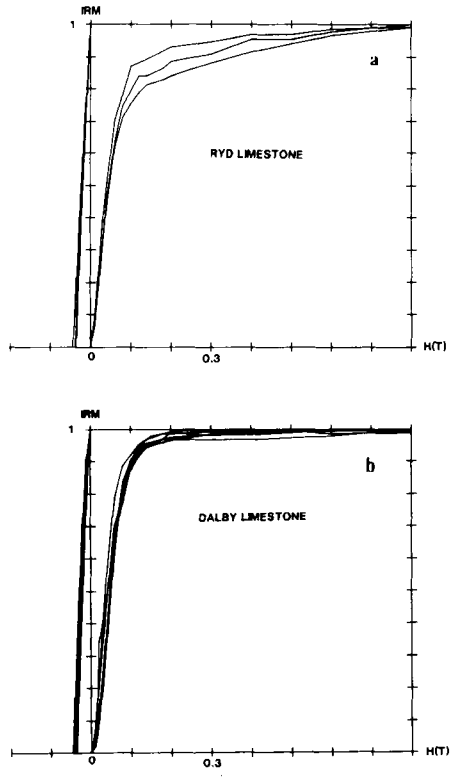

Figure 11. Normalized IRM curves from the Ryd (a) and Dalby (b) limestone.

is totally unblocked by temperatures of 550°–570 °C. In other cases however, the total IRM is composite (e.g. example Bg in Fig. 12a), showing variable low- and high-coercivity phases unblocking below 400 °C. Subsequently, a high unblocking temperature component, resident in the low-coercivity axis, is removed in the 400°–550 °C range. This behaviour can be interpreted in terms of a mixture of low- and high-coercivity magnetite (>0.2 T saturation field) although the presence of pyrrhotite, unblocking between 150° and 400 °C cannot be discounted.

Dark grey limestones from the Holen limestone show similar composite behaviour, but with increased influence of the high-coercivity phase (example Dg in Fig. 12 a and c). A low-coercivity component is unblocked below 150 °C followed by mixed low- and high-field components unblocked until 570 °C. In this case, a high-coercivity phase is identified above 570 °C, and resident in fine-grained and high-coercivity magnetite (Fig. 12c). We interpret this behaviour to indicate magnetite of varying grain-size [note that example Dg in Fig. 13 corresponds to the sample in Fig. 6(b)].

Red and red/grey samples demonstrate multivectorial behaviour during demagnetization of the composite IRM. In most cases, both low- and high-coercivity phases are unblocked below 400°–500 °C, predominantly low-coercivity phases to 570°–590 °C, and finally the high-coercivity phase is isolated above 590°–610 °C. In these samples, the high-coercivity magnetization clearly resides in haematite (Fig. 12a and c) unblocking up to 630 °C. Haematite is therefore present as a subordinate remanence carrying phase in these experiments. Continuous thermal decay curves and almost complete unblocking below 600 °C suggest a single-domain *pigmentary* haematite paragenesis (Collinson 1974).

Thermomagnetic analysis

Thermomagnetic experiments were conducted on a Curie balance using a field of 0.5 T. Heating/cooling cycles were performed in air.

Red samples of Holen limestone contain variable proportions of magnetite and haematite as evidenced from Curie temperatures of the order of 560°–580° and 660°–680° respectively (Fig. 13b). Heating and cooling curves are fairly reversible, but minor increases in saturation magnetization are noticed.

Thermomagnetic behaviour is variable within the Gullhögen limestone. For example, some variegated red and grey samples reveal only haematite during the heating cycle, whereas both haematite and magnetite are recognizable during cooling (Fig. 13a). This suggests magnetite production during heating. The haematite Curie temperature is often 'supressed' during cooling (Fig. 13a), which may suggest formation of secondary magnetite due to reduction of haematite.

In grey limestones, the paramagnetic contribution is dominant and Curie points are difficult to identify. No indication of haematite is detected however (Fig. 13c and

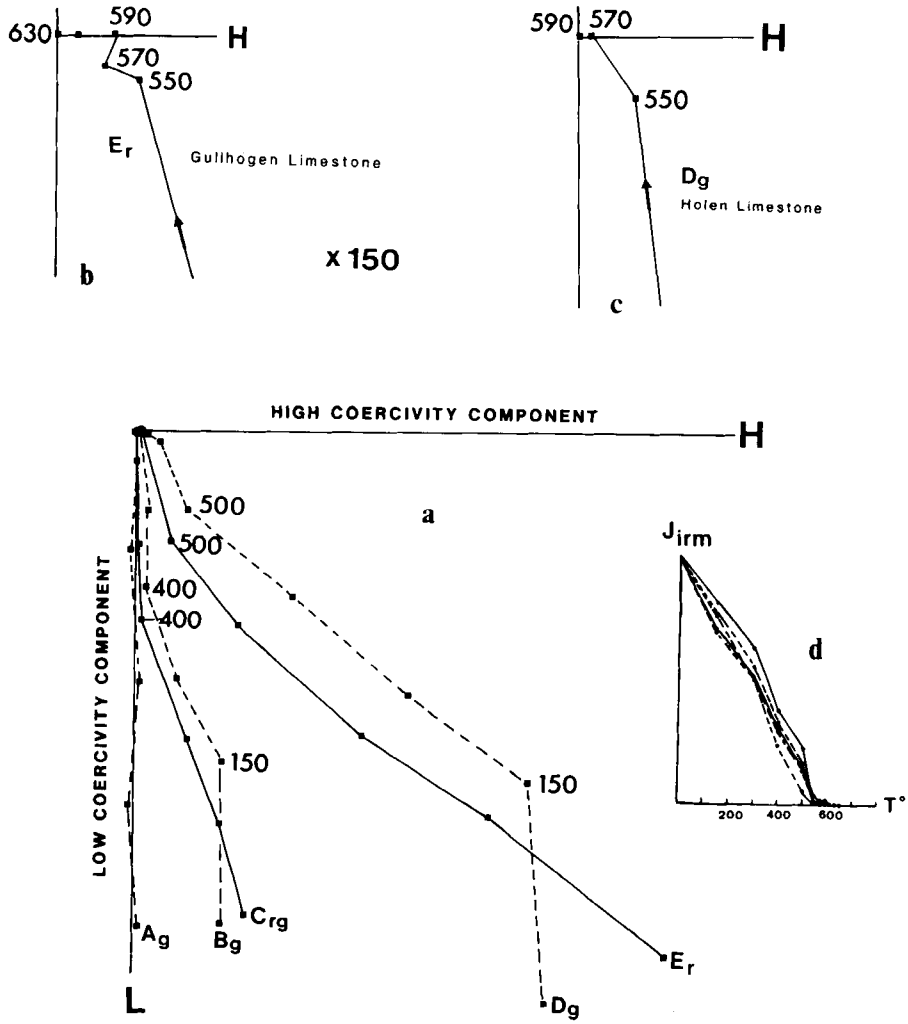

Figure 12. (a) Thermal demagnetization (vector plot) of composite IRM, i.e. 0.8 and 0.2 T induced along the horizontal and vertical axis respectively (*cf.* text). Sublettering g, rg and r denote grey, variegated red and grey and red limestone respectively. (b) and (c) are expanded diagrams (150 times) of example Er and Dg in (a). (d) Normalized IRM decay curves. Solid lines = red or variegated red and grey samples; stippled lines = grey samples.

d). Heating and cooling curves show a low radius of curvature which may suggest the presence of very fine-grained (SD) magnetite. Secondary magnetite is seen on almost all cooling curves (*cf.* Fig. 13d). In the grey Dalby limestone, the presence of pyrrhotite is indicated from irreversible 'Curie temperatures' of around 320 °C (Fig. 13c). Pyrrhotite is inferred to carry parts of the IB component since some samples from the Dalby limestone show pronounced unblocking between 300° and 350 °C during thermal demagnetization.

DISCUSSION

Remanence carriers

The remanence properties of the examined limestones are almost entirely governed by magnetite with only accessory haematite. In grey limestones, IRM experiments (e.g. Dalby limestone, section III) suggest that some magnetite grains are in a single- or pseudo-single-domain state. This also appears to be the case for red or variegated red and grey limestones, but in addition pigmentary haematite can be of importance. Haematite has also been identified along sedimentary discontinuity surfaces along with goethite, pyrite, glauconite and phosphorite forming mineralized surface crusts (Lindström 1963).

Pigmentary haematite is probably early diagenetic in origin and may in part have formed from a goethite precursor (*cf.* Lowrie & Heller 1982). Conversely, magnetite may have a detrital, biological and/or diagenetic origin. Nevertheless, a primary or *early* diagenetic origin is inferred from the stratigraphically related polarity pattern. However, a few grey sample from the Holen limestone (Level 2), exhibit dual-polarity HB directions at sample level. Thermomagnetic analysis, composite IRM analysis (Fig. 12c) and palaeomagnetic experiments (Fig. 6b) suggest that both polarities reside in magnetite. We interpret the polarity during deposition to be reverse (Zone R1), and the superimposed HB normal polarity direction may therefore have originated by:

(1) pDRM/bioturbation;
(2) growth of 'non-magnetic' magnetite through the

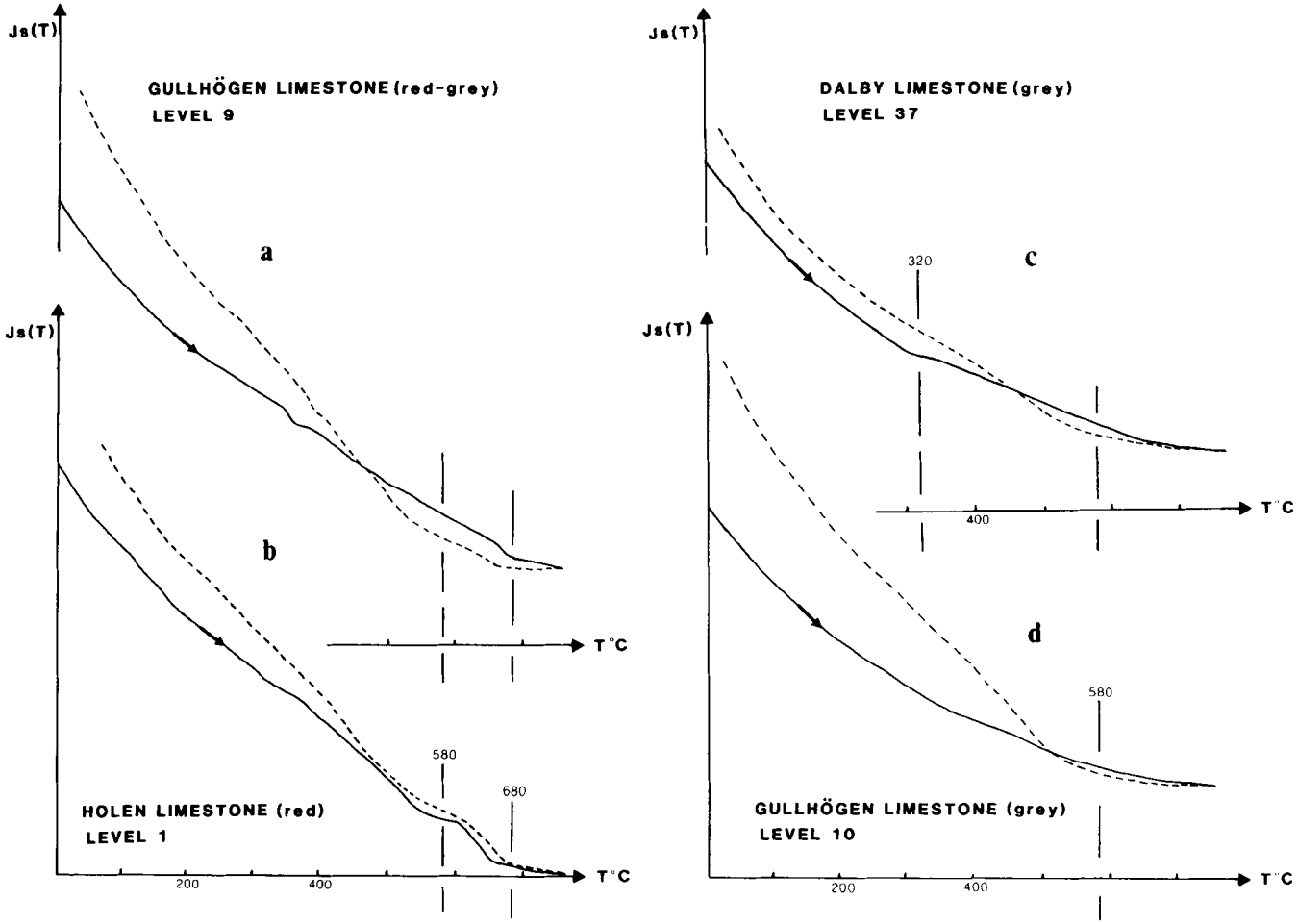

Figure 13. Thermomagnetic analyses of samples from the (a) Gullhögen, (b) Holen, (c) Dalby and (d) Gullhögen limestones.

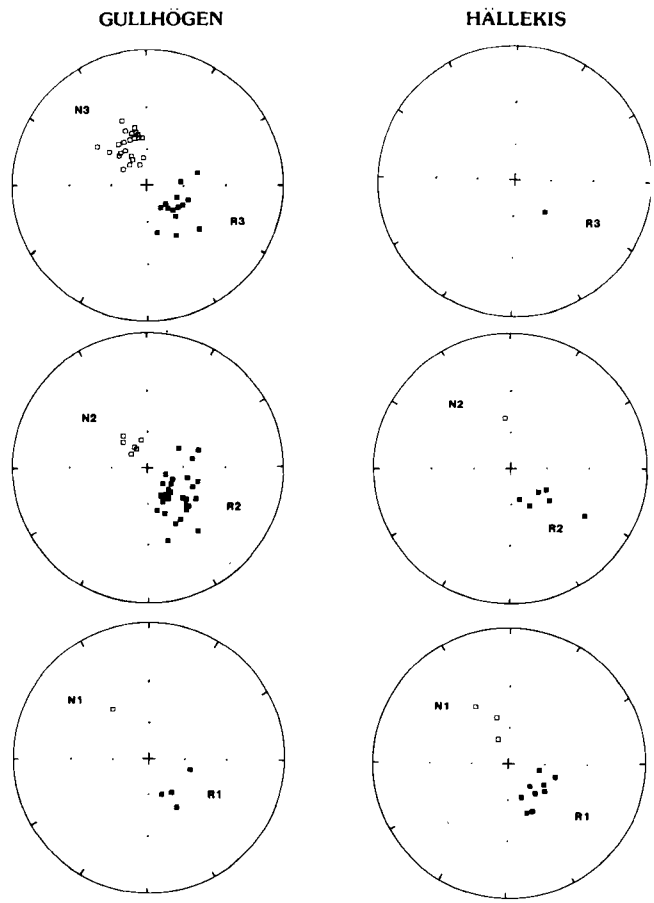

superparamagnetic single-domain threshold size, e.g. magnetite precipitation by bacteria; or

(3) secondary formation of single-domain magnetite from a different mineral precursor, e.g. during diagenesis.

Due to the lack of thorough bioturbation across the discontinuity surface between the Holen and the overlying Skövde limestone (Holmer 1983) we favour either the second or third alternative.

Ordovician magnetostratigraphy

The identification of straigraphically linked polarity intervals of the HB component allows a preliminary polarity time-scale to be constructed for Llanvirn–Caradoc times (Fig. 4). This polarity zonation is substantiated by repeatability on a local scale i.e. samples from each level always display the same polarity. Some complications are evident however, notably that both polarities of HB locally occur in single samples of the top Holen limestone. Furthermore, discontinuities representing considerable time-gaps exist within the sampled sections (Figs 3–4).

To explore the regional repeatability of the postulated polarity zonation, a comparison is made with results from Hällekis on Mount Kinnekulle (Fig. 2a and c) listed by

Figure 14. Distribution of characteristic HB components from Gullhögen quarry (left) and the Hällekis area (*cf.* text). Data are divided into stratigraphically linked polarity zones N1–N3 and R1–R3.

Claesson (1977) and re-evaluated by Torsvik & Trench (1991). Directions of component HB are plotted for both localities in Fig. 14. At Hällekis, three normal polarity directions are observed at the stratigraphic equivalent to the upper part of the Holen limestone, referred to as top Kunda (*cf.* Fig. 3) by Claesson (1977). This strengthens the postulate of N1 from Gullhögen. N1, however, appears to be a short-lived zone, and at Gullhögen, zone N1 is argued to have been concealed by the sedimentary break between the Holen and Vamb limestone. In addition, *one* normal polarity direction reported within the Gullhögen formation at Hällekis corresponds to N2 in the same lithology at the Gullhögen quarry. Hence, the Hällekis results, although of only moderate data quality (Torsvik & Trench 1991) sustain the N1, R1, N2, R2 and R3 data from Gullhögen quarry. Sampling in the Hällekis section did not reach zone N3.

Combining the palaeomagnetic results from Gullhögen with earlier studies in Scandinavia (Torsvik *et al.* 1990b; Torsvik & Trench 1990; Perroud *et al.* 1991) suggests an Ordovician magnetostratigraphy as follows (Fig. 15):

(1) Tremadoc, Arenig and Early Llanvirn times were characterized by dominantly reverse polarity (zone R1);

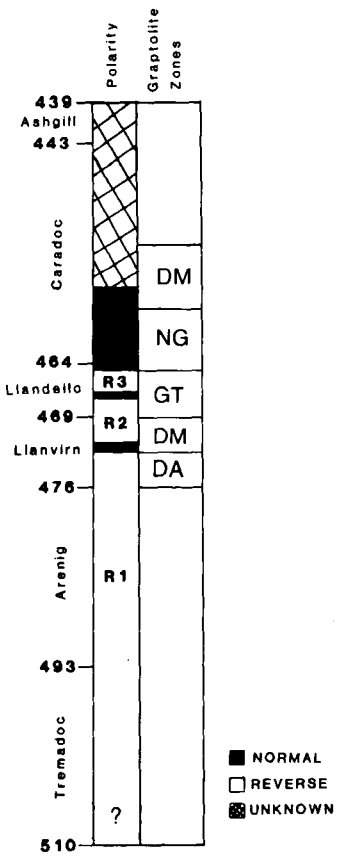

Figure 15. A suggested Ordovician polarity pattern based on palaeomagnetic data from Scandinavia. Approximate absolute ages are taken from Harland *et al.* (1989). Graptolite zones with relevance to the present study after Jaanusson (1982a) and Holmer (1989). DA = Didymograptus artus; DM = Didymograptus murchisoni; GT = Glyptograptus teretiusculus; NG = Nemagraptus gracilis; DM = Dipolograptus multidens.

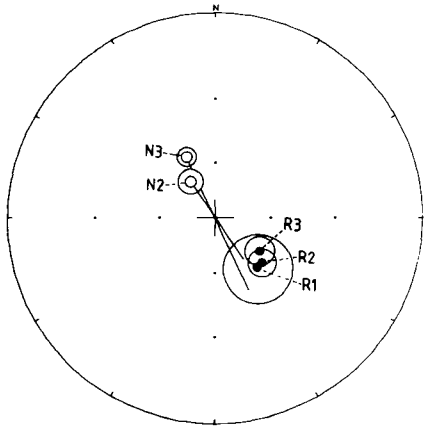

Figure 16. Polarity zone means (N2 and N3 and R1–R3) and their associated a_{95} confidence errors (see Table 1).

(2) a normal polarity zone (zone N1) is identified in mid–Upper Llanvirn times;

(3) late Llanvirn to mid-Llandeilo was once more of reverse polarity (zone R2), followed by;

(4) a normal polarity zone (zone N2) in mid-Llandeilo times;

(5) further reverse polarity prevailed until late Llandeilo times (zone R3); and

(6) the Late Landeilo to mid-Caradoc was characterized by normal polarity (zone N3). The upward extent of this normal polarity zone is as yet unknown.

Apparent polar wander and palaeogeography

Normal and reverse field directions are broadly antipodal (NW up, SE down), which suggests that the geomagnetic field was axial-symmetrical in Ordovician times (Fig. 16—Table 1). A reversal test (McFadden & Lowes 1981), comparing the N1–N2 and R1–R3 zones shows that these directions share a common mean at the 95 per cent confidence level. However, the zone N3 mean direction proves different from R3 at the same confidence level which may relate to APW. Indeed, there is a systematic shift in both declination and inclination throughout the Lower–Middle Caradoc (zone N3, Fig. 17). This shift, toward more northerly declinations and shallower upward dipping inclinations, cannot be attributed to contamination caused by Permo-Carboniferous overprinting (IB component).

Mid-Llanvirn–Upper Llandeilo palaeomagnetic results (N1 and N2, R1–R3) yield a mean pole of N14 and EO49 (Table 2, Fig. 18), whereas Lower Caradoc (N3) data yield a pole of N5 and EO34. In Fig. 19 we have also included Arenig–Llanvirn results from southern Sweden (Perroud *et al.* 1991) and a Tremadoc pole from northern Norway (Torsvik *et al.* 1990b). The collective data, Tremadoc to mid-Caradoc, define a systematic westerly APW shift (Fig. 18), which is interpreted to represent counter-clockwise rotation of Baltica. Rotation was probably initiated in Upper Cambrian–Lower Ordovician (Tremadoc) times, coeval with the 'Finnmarkian' orogeny in the Northern Scandinavian Caledonides (Torsvik *et al.* 1991). An apparent 'stillstand' is observed during Arenig and Llanvirn times, followed by renewed counter-clockwise rotation in

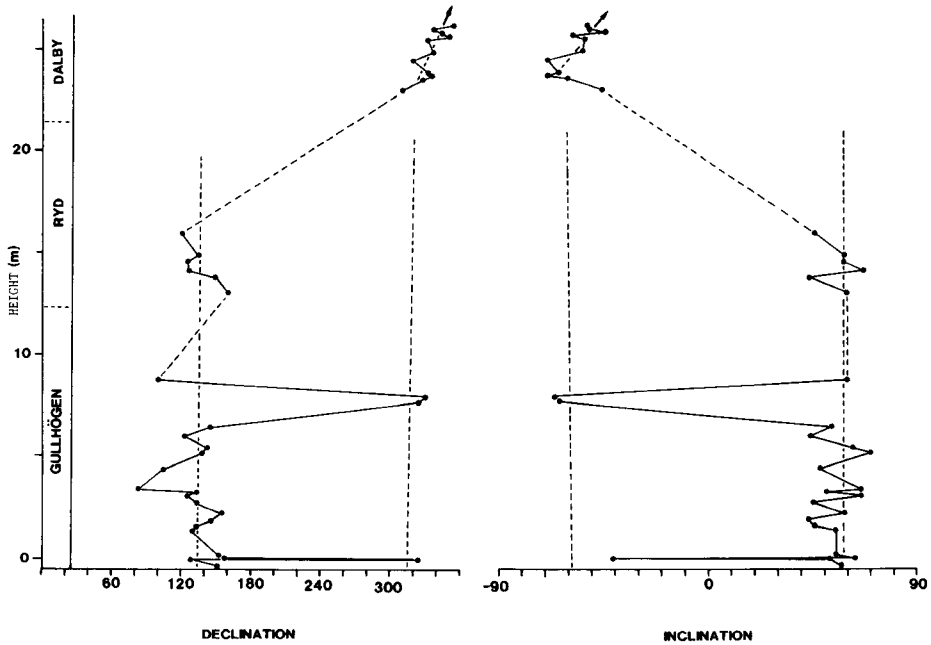

Figure 17. Mean declination and inclination calculated for each sampling level. Stippled lines represent average declination (132°/312°) and inclinations (±58°) for the Llanvirn–Llandeilo sections (see Table 2). Note the systematic trend in both declination and inclination in lower Caradoc (Dalby limestone) times.

Table 1. Palaeomagnetic results from the Gullhøgen Quarry, Skøvde.

PZ	Dec	Inc	N	a95	k	Age
High-Blocking Components:						
R1	140	+55	4	17.3	29.2	M LLANVIRN
N1	324	-41	1			M LLANVIRN
R2	134	+55	29	7.1	15.2	M LLANVIRN - M LLANDEILO
N2	326	-66	6	6.6	104.2	M LLANDEILO
R3	127	+60	15	7.7	25.9	M LLANDEILO - U LLANDEILO
N3	335	-54	24	4.8	39.6	U LLANDEILO - M CARADOC
Intermediate Blocking Components:						
I-III	198	-10	123	2.0	41.9	Permo-Carb. overprint
	(VGP - N35 & E171, dp/dm=1/2)					(c. 287±14 Ma)

PZ=Polarity Zone; Dec=Mean Declination; Inc=Mean Inclination; N=Number of samples; a95=95 percent confidence circle; k=precision parameter;

Geographic Sampling Location: Lat=N58.3, Long=E13.9

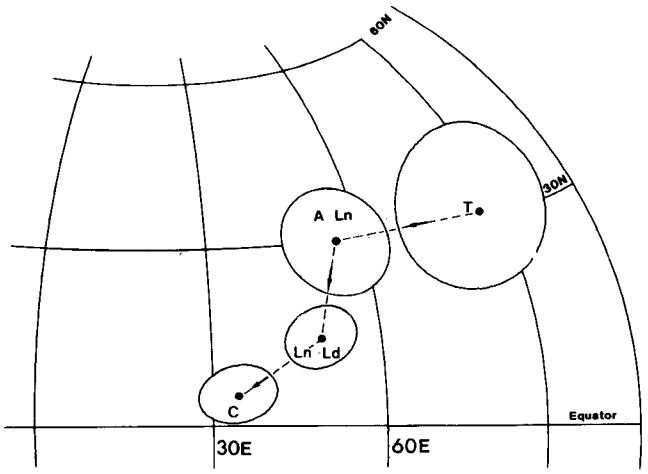

Figure 18. Distribution of the most 'reliable' Tremadoc to Caradoc palaeomagnetic poles from Scandinavia. T = pole 1 (Table 2); A–Ln = pole 4; Ln–Ld = pole 5; C = pole 6. Poles are shown with *dp/dm* ovals except the A–Ln pole which is shown with A_{95} error confidence. Equal-area projection.

Llandeilo and Caradoc times (Fig. 19). Northward latitudinal drift is also recognized in post-Llanvirn times, hence indicating Baltica's approach to temperate-equatorial conditions in Late Ordovician, Caradoc–Ashgill, times (Fig. 19).

This palaeogeographic scenario concurs with palaeoclimatic indicators as warm water carbonates are only recognized in the central confacies belt in Ashgill times (Webby 1980). Similarly, one might expect continental rotation to change the palaeo-orientation of confacies belts with time. For example, if the boundaries are climate-controlled, higher faunal provinciality should prevail during the Lower Ordovician when the confacies belts were E–W orientated (Fig. 19). A systematic study of the changes in faunal/facies patterns across Baltoscandia in Ordovician times may reveal a link to the continental rotation documented here.

Table 2. Ordovician palaeomagnetic results, northern Norway and southern Sweden.

Age	Dec	Inc	N	a95	k	Lat	Long	dp/dm	Pol
Tremadoc[1]	104	+57	10	10.6	21.6	N31	E086	11/15	R
Arenig-Llanvirn[2]	132	+70	73	2.2	58.0	N30	E046	3/4	R
Arenig-Llanvirn[3]	138	+62	6#	5.1	176	N18	E046	6/8	R
Arenig-Llanvirn[4]			4#	9.0*		N30	E055		R
M Llanvirn-U Llandeilo[5]	134	+58	55	4.4	19.6	N14	E049	5/6	M
U Llandeilo-M Caradoc[6]	335	-54	24	4.8	39.6	N05	E034	5/7	N

Lat=VGP latitude; Long=VGP longitude; dp/dm=semi-axis of the oval of the 95 percent confidence about the mean pole; N=number of samples (sites/areas)#; *A95; Pol=Polarity, R=Reverse, N=Normal & M=Mixed (cf. Table 1 for further legend).

[1]Torsvik et al. (1990b)
[2]Claesson (1978)
[3]Torsvik & Trench (1990)
[4]Perroud et al. (1991)
Note - This pole has been used in Fig. 18 and also used to position Baltica in Arenig-Llanvirn times (Fig. 19).
[5]This study (N1+N2 & R1-R3)
[6]This study (N3)

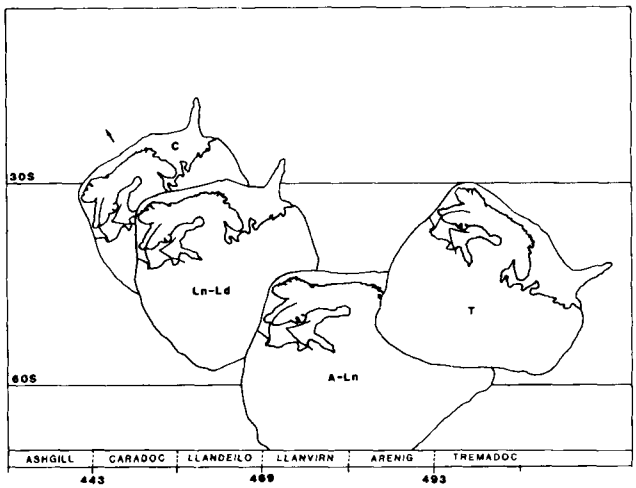

Figure 19. Ordovician palaeotectonic scenario for Baltica based on poles shown in Fig. 18. Approximate ages (not to scale) after Harland *et al.* (1989). The palaeo-orientation of the Central Confacies Belt (see Fig. 1a) is indicated. Galls projection.

ACKNOWLEDGMENTS

THT (AT) thanks NAVF (NERC) for financial support. Norwegian Lithosphere project contribution 133.

REFERENCES

Claesson, K. C., 1977. Palaeomagnetic studies of Swedish Lower Palaeozoic rocks, *PhD thesis*, University of Newcastle.

Claesson, K. C., 1978. Swedish Ordovician Limestones: Problems in clarifying their directions of magnetization, *Phys. Earth planet. Inter.*, **16**, 65–72.

Collinson, D. W., 1974. The role of pigment and specularite in the remanent magnetism of red sandstones, *Geophys. J. R. astr. Soc.*, **38**, 253–264.

Harland, W. B., Armstrong, R. L., Cox, A. V., Craig, L. E., Smith, A. G. & Smith, D. G., 1989. *A Geological Time Scale*, Cambridge University Press, Cambridge, UK.

Holmer, L. E., 1983. Lower Viruan discontinuity surfaces in central Sweden, *Geologiska Foreningens i Stockholm Forhandlinger*, **105**, 29–42.

Holmer, L. E., 1989. Middle Ordovician phosphatic inarticulate brachiopods from Vastergotland and Dalarna, Sweden, *Fossils Strata*, **26**, 1–172.

Jaanusson, V., 1964. The Viruan (Middle Ordovician) of Kinekulle and northern Billingen, *Bull. Geol. Inst. Univ. Uppsala*, **43**, 1–73.

Jaanusson, V., 1976. Faunal dynamics in the middle Ordovician (Viruan) of Balto-Scandia, in *The Ordovician System. Proceedings of a Palaeontological Association Symposium*, pp. 301–326, ed. Basset, M. G., University of Wales Press, Cardiff.

Jaanusson, V., 1982a. Introduction to the Ordovician of Sweden, *Paleont. Contrib. Univ. Oslo*, **279**, 1–10.

Jaanusson, V., 1982b. Ordovician of Vastergotland, *Paleont. Contrib. Univ. Oslo*, **279**, 164–183.

Lindström, M., 1963. Sedimentary folds and the development of limestone in an early Ordovician sea, *Sedimentology*, **2**, 243–292.

Lindström, M., 1971. Vom Anfang, Hochstand und Ende eines epikontinentalmeeres, *Geol. Rundschau.*, **60**, 419–438.

Lowrie, W. & Heller, F., 1982. Magnetic properties of Marine Limestones, *Rev. Geophys. Space Phys.*, **20**, 171–192.

McCabe, C. & Channell, J. E. T., 1990. Palaeomagnetic results from volcanic rocks of the Shelve Inlier, Wales: evidence for a wide late Ordovician Iapetus Ocean in Britain, *Earth planet. Sci. Lett.*, **96**, 458–468.

McFadden, P. L. & Lowes, F. J., 1981. The discrimination of mean directions drawn from Fisher distributions, *Geophys. J. R. astr. Soc.*, **67**, 19–33.

Mulder, F. G., 1971. Paleomagnetic research in some parts of Central and Southern Sweden, *Sveriges Geologiska Undersøkning, Series C*, **653**, 64, 10, 1–64.

Palma, L., 1967. O perekhodnoy polose mezhdu severoy i osevoy fatsial'nymi zonami ordovika pribaltika, *Eesti NSV Tead. Akad. Toim., Keemia Geol.*, **16**, 272–275 (in Russian with English summary).

Perroud, H., Robardet, M. & Bruton, D. L., 1991. Palaeomagnetic constraints upon the paleogeographic position of the Baltic Shield in Ordovician, *Tectonophysics*, in press.

Thorslund, P., 1962. Kambro-siluravlagringar utanfor fjall-kedjan, *Sver. Geol. Unders. Ser. Ba*, **16**, 113–153.

Thorslund, P. & Jaanusson, V., 1960. The Cambrian, Ordovician and Silurian in Vastergotland, Narke, Dalarna and Jamtland, central Sweden, *Guide to Excursions Nos. A23 and C18*, pp. 1–51, International Geological Congress XXI Session, Norden 1960, Sweden, Guide book e, Stockholm

Torsvik, T. H. & Trench, A., 1991. The Lower-Middle Ordovician palaeofield of Scandinavia: southern Sweden 'revisited', *Phys. Earth planet. Inter.*, **65**, 283–291.

Torsvik, T. H., Smethurst, M. A., Briden, J. C. & Sturt, B. A., 1990a. A review of Palaeozoic palaeomagnetic data from Europe and their palaeogeographical implications, in *Palaeogeography and Biogeography*, Geological Society of London Memoir, vol. 12, pp. 25–41, eds McKerrow, W. S. & Scotese, C. R.

Torsvik, T. H., Olesen, O., Ryan, P. D. & Trench, A., 1990b. On the paleogeography of Baltica during the Palaeozoic: new palaeomagnetic data from the Scandinavian Caledonides, *Geophys. J. Int.*, **103**, 261–279.

Torsvik, T. H., Ryan, P. D., Trench, A. & Harper, D. A. T., 1991. Cambrian-Ordovician palaeogeography of Baltica, *Geology*, **19**, 7–10.

Trench, A., Torsvik, T. H., Smethurst, M. A., Woodcock, N. H. & Metcalfe, R., 1991. A palaeomagnetic study of the Builth Wells–Llandrindod Wells Ordovician inlier, Wales: palaeogeographic and structural implications, *Geophys. J. Int.*, **105**, 477–489.

Watts, D. & Briden, J. C., 1984. Palaeomagnetic signature of slow post-orogenic cooling of the north-east Highlands of Scotland recorded in the Newer Gabbros of Aberdeenshire, *Geophys. J. R. astr. Soc.*, **77**, 775–788.

Webby, B. D., 1980. Biogeography of Ordovician stromatoporoids, *Paleogeog. Palaeoclimat. Palaeoecol.*, **32**, 1–19.